Journal of Solid State Chemistry 194 (2012) 113–118

Contents lists available at SciVerse ScienceDirect

Journal of Solid State Chemistry

journal homepage: www.elsevier.com/locate/jssc

Crystal structure, electrical resistivity, and X-ray photoelectron spectroscopy of $BaAg_2As_2$

Stanislav S. Stoyko, Peter E.R. Blanchard, Arthur Mar*

Department of Chemistry, University of Alberta, Edmonton, Alberta, Canada T6G 2G2

ARTICLE INFO

Article history:
Received 15 March 2012
Received in revised form
28 April 2012
Accepted 6 May 2012
Available online 14 May 2012

Keywords:
Barium
Silver
Arsenide
Electronic structure
Electrical resistivity
X-ray photoelectron spectroscopy

ABSTRACT

The ternary arsenide $BaAg_2As_2$ has been prepared by reaction of the elements at 850 °C. Single-crystal and powder X-ray diffraction analysis revealed that it adopts the $ThCr_2Si_2$-type structure (Pearson symbol *tI*10, space group *I*4/*mmm*, $Z=2$, $a=4.6025(3)$ Å, $c=10.8672(6)$ Å at 295 K) featuring $[Ag_2As_2]$ layers interconnected by homoatomic As–As bonds along the *c*-direction. Band structure calculations indicate no gap at the Fermi level, and support the occurrence of strong As–As and weak Ag–Ag bonding. The asymmetric lineshape and the absence of a BE shift in the Ag $3d_{5/2}$ core-line peak relative to the element suggest delocalization of the Ag valence electrons. A significant negative BE shift (1.0 eV) in the As $3d_{5/2}$ core-line peak relative to the element confirms the presence of anionic As atoms. A reversible transition is observed at 175 K in the electrical resistivity, and is probably related to a structural phase transition.

1. Introduction

Numerous intermetallic compounds with the general formula AM_2X_2 (A=alkaline-earth or rare-earth metal, M=transition metal, X=group 13–15 element) are known [1]. The vast majority of them adopt the tetragonal $ThCr_2Si_2$-type structure, whereas a smaller fraction adopt the tetragonal $CaBe_2Ge_2$- or trigonal $CaAl_2Si_2$-type structures. Considerable effort is currently focused on characterizing the physical properties of ternary barium transition-metal pnictides BaM_2Pn_2 and especially the arsenides BaM_2As_2, given the discovery of superconductivity in doped $BaFe_2As_2$ [2,3]. The arsenide series is extensive for the 3d metals (M=Cr–Zn with $ThCr_2Si_2$-type structure) [4–8], less so for 4d metals (M=Ru–Pd with $ThCr_2Si_2$-type structure; M=Cd with $CaAl_2Si_2$-type structure) [8–14], and limited for 5d metals (M=Pt with $CaBe_2Ge_2$-type structure) [15]. ($BaZn_2As_2$ and $BaPd_2As_2$ also form other polymorphs [8,10,13].) The M=Ag member is apparently absent so far, and it is of interest to determine which structure type it would adopt.

In the course of investigating the silver-containing systems A–Ag–As (where A is a divalent electropositive metal), attempts to prepare the Ba analogue of the $CaCu_4P_2$-type phases AAg_4As_2 (A=Sr, Eu) [16] yielded instead the heretofore missing silver member of the BaM_2As_2 series. Here we report on the crystal structure, electrical resistivity, and XPS studies on $BaAg_2As_2$, and we present evidence for the occurrence of a low-temperature phase transition.

2. Experimental

2.1. Synthesis

Stoichiometric mixtures of freshly scraped Ba pieces (99.8%, Alfa-Aesar), Ag powder (99.99%, Aldrich), and As lumps (99.999%, Alfa-Aesar) were loaded into alumina crucibles placed within fused-silica tubes, which were evacuated and sealed. The tubes were heated to 850 °C over 2d, held at that temperature for 2d, cooled to 800 °C over 1d, held at that temperature for 7d, and cooled to room temperature over 2d. These reactions yielded highly crystalline $BaAg_2As_2$ samples that were single-phase, as confirmed by powder X-ray diffraction patterns (Fig. 1) collected on an Inel diffractometer equipped with a position-sensitive detector (CPS 120) and a Cu $K_{\alpha 1}$ radiation source. Large irregularly shaped crystals (Fig. S1 in Supplementary Data) were found to have an average composition of 21(1)% Ba, 37(1)% Ag, and 42(2)% As, as determined by energy-dispersive X-ray (EDX) analysis on a Zeiss EVO MA 15 scanning electron microscope, in good agreement with the expected composition.

2.2. Structure determination

Intensity data were collected at 295 K on a Bruker D8 diffractometer equipped with a SMART APEX II CCD area detector and a Mo K_α radiation source, using ω scans at 6 different ϕ angles with

---

* Corresponding author. Fax: +1 780 492 8231.
E-mail address: arthur.mar@ualberta.ca (A. Mar).

0022-4596/$ - see front matter © 2012 Elsevier Inc. All rights reserved.
http://dx.doi.org/10.1016/j.jssc.2012.05.003

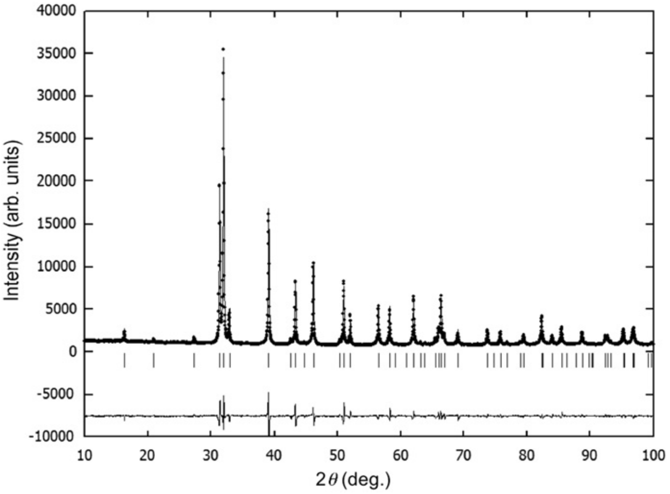

Fig. 1. Powder XRD pattern for $BaAg_2As_2$. The observed profile is indicated by filled circles and the calculated profile by the solid line. Bragg peak positions are marked by the tic marks. The difference plot is shown at the bottom.

Table 1
Crystallographic data for $BaAg_2As_2$.

Data collection and refinement	
Formula	$BaAg_2As_2$
Formula mass (amu)	502.92
Space group	*I*4/*mmm* (No. 139)
a (Å)	4.6025(3)
c (Å)	10.8672(6)
V (Å^3)	230.20(2)
Z	2
ρ_{calcd} (g cm^{-3})	7.256
T (K)	295(2)
Crystal dimensions (mm)	$0.08 \times 0.13 \times 0.15$
Radiation	Graphite monochromated Mo K_α, $\lambda = 0.71073$ Å
μ(Mo K_α) (mm^{-1})	30.94
Transmission factors	0.070–0.220
2θ limits	7.50°–66.14°
Data collected	$-6 \leq h \leq 6$, $-6 \leq k \leq 6$, $-16 \leq l \leq 16$
No. of data collected	1605
No. of unique data, including $F_o^2 < 0$	154 ($R_{int} = 0.021$)
No. of unique data, with $F_o^2 > 2\sigma(F_o^2)$	154
No. of variables	9
$R(F)$ for $F_o^2 > 2\sigma(F_o^2)$ [a]	0.014
$R_w(F_o^2)$ [b]	0.049
Goodness of fit	1.31
$(\Delta\rho)_{max}$, $(\Delta\rho)_{min}$ (e Å^{-3})	1.03, −0.82
Positional and displacement parameters [c]	
Ba at 2*a* (0, 0, 0)	
U_{eq} (Å^2)	0.0150(2)
Ag at 4*d* (0, ½, ¼)	
U_{eq} (Å^2)	0.0267(2)
As at 4*e* (0, 0, *z*)	
z	0.38420(6)
U_{eq} (Å^2)	0.0175(2)
Interatomic distances (Å)	
Ba–As (× 8)	3.4893(3)
Ba–Ag (× 8)	3.5604(2)
Ag–As (× 4)	2.7244(4)
Ag–Ag (× 4)	3.2545(2)
As–As	2.5169(13)

[a] $R(F) = \sum ||F_o| - |F_c|| / \sum |F_o|$.

[b] $R_w(F_o^2) = [\sum[w(F_o^2 - F_c^2)^2] / \sum wF_o^4]^{1/2}$; $w^{-1} = [\sigma^2(F_o^2) + (Ap)^2 + Bp]$ where $p = [\max(F_o^2, 0) + 2F_c^2]/3$.

[c] U_{eq} is defined as one-third of the trace of the orthogonalized U_{ij} tensor.

a frame width of 0.3° and an exposure time of 15 s per frame. Face-indexed numerical absorption corrections were applied. Structure solution and refinement were carried out with use of the SHELXTL (version 6.12) program package [17]. The centrosymmetric space group *I*4/*mmm* was chosen, initial positions (standardized by STRUCTURE TIDY [18]) for all atoms were located by direct methods, and refinements proceeded in a straightforward manner in accordance with the $ThCr_2Si_2$-type structure. When individually freed, the occupancies of the atomic sites converged to 1.022(3) for Ba, 0.966(2) for Ag, and 1.015(5) for As. The Ba and As sites were assumed to be fully occupied, as no improvements in the agreement factors were observed and the slight overoccupancies can probably be attributed to errors in the absorption correction. Introducing the small Ag substoichiometry led to a noticeable improvement in agreement factors ($R(F)$ decreased from 0.014 to 0.011, and $R_w(F^2)$ from 0.049 to 0.028). If the Hamilton *R*-test is applied [19], the *R*-factor ratio of $0.014/0.011 = 1.27$ exceeds the significance point of 1.02 at the 0.5% significance level, indicating that this improvement is meaningful. The EDX analysis presented above does suggest a deficiency in Ag ("$BaAg_{1.76}As_2$") that seems to be consistent with the model refined here ("$BaAg_{1.93}As_2$"), but care should be exercised in accepting this conclusion because uncertainties in EDX analyses are often underestimated. A further argument in favour of this model is that substoichiometry of the transition metal component is observed in $BaCu_{1.88}As_2$ with the same $ThCr_2Si_2$-type structure [7] and $BaAg_{1.84}Bi_2$ with the closely related $CaBe_2Ge_2$-type structure [20]. On the other hand, inspection of the powder XRD patterns did not reveal the presence of excess Ag or other secondary phases, at least within the detection limit of this technique and its restriction to crystalline material. At this stage, we must admit the possibility that a small degree of Ag substoichiometry is likely, but more definitive experimental evidence remains to be gathered. For simplicity in subsequent discussion, we opt to retain the fully stoichiometric model. Crystallographic details are summarized in Table 1. Further data, in CIF format, have been sent to Fachinformationszentrum Karlsruhe, Abt. PROKA, 76344 Eggenstein–Leopoldshafen, Germany, as supplementary material No. CSD-424361 and can be obtained by contacting FIZ (quoting the article details and the corresponding CSD numbers).

In light of the low-temperature transition identified later in the measurement of electrical resistivity, intensity data were recollected on the same crystal at 148 K. At this temperature, the unit cell constants are $a = 4.6082(7)$ Å, $c = 10.751(3)$ Å, and $V = 228.30(8)$ Å^3. However, significant difficulties were encountered in developing a suitable structural model. Refinement of the room-temperature model ($ThCr_2Si_2$-type) led to poor agreement factors ($R(F) = 0.111$, $R_w(F^2) = 0.259$) and a large peak in the difference electron density map (19.8 e$^-$ Å^{-3}) close to the Ba site. Attempts to introduce structural distortions in other space groups (including those in lower symmetry than tetragonal) failed. Examination of the intensity patterns suggested only a weak violation of the *I*-centring condition (e.g., very weak 100 reflections seen in the *hk*0 net at 148 K) (Fig. S2 in Supplementary Data). Further work is in progress to characterize the low-temperature structure.

2.3. Band structure calculations

Tight-binding linear muffin tin orbital band structure calculations were performed on $BaAg_2As_2$ within the local density and atomic spheres approximation with use of the Stuttgart TB-LMTO-ASA program (version 4.7) [21]. The basis set consisted of Ba 6s/5d/6p, Ag 5s/4d/5p, and As 4s/4p/4d orbitals, with the Ba 6p